

REPORT DOCUMENTATION PAGE			Form Approved OMB NO. 0704-0188		
<p>The public reporting burden for this collection of information is estimated to average 1 hour per response, including the time for reviewing instructions, searching existing data sources, gathering and maintaining the data needed, and completing and reviewing the collection of information. Send comments regarding this burden estimate or any other aspect of this collection of information, including suggestions for reducing this burden, to Washington Headquarters Services, Directorate for Information Operations and Reports, 1215 Jefferson Davis Highway, Suite 1204, Arlington VA, 22202-4302. Respondents should be aware that notwithstanding any other provision of law, no person shall be subject to any penalty for failing to comply with a collection of information if it does not display a currently valid OMB control number.</p> <p>PLEASE DO NOT RETURN YOUR FORM TO THE ABOVE ADDRESS.</p>					
1. REPORT DATE (DD-MM-YYYY) 02-05-2011		2. REPORT TYPE Final Report		3. DATES COVERED (From - To) 25-Sep-2003 - 24-Sep-2009	
4. TITLE AND SUBTITLE BIOLOGICALLY INSPIRED STRATEGIES, ALGORITHMS AND HARDWARE FOR VISUAL GUIDANCE OF AUTONOMOUS HELICOPTERS			5a. CONTRACT NUMBER DAAD19-03-1-0359		
			5b. GRANT NUMBER		
			5c. PROGRAM ELEMENT NUMBER 611102		
6. AUTHORS Mandyam V. Srinivasan, Michael Ibbotson			5d. PROJECT NUMBER		
			5e. TASK NUMBER		
			5f. WORK UNIT NUMBER		
7. PERFORMING ORGANIZATION NAMES AND ADDRESSES Australian National University Australian National University Cnr of Barry Drive and North Road 2600 -			8. PERFORMING ORGANIZATION REPORT NUMBER		
9. SPONSORING/MONITORING AGENCY NAME(S) AND ADDRESS(ES) U.S. Army Research Office P.O. Box 12211 Research Triangle Park, NC 27709-2211			10. SPONSOR/MONITOR'S ACRONYM(S) ARO		
			11. SPONSOR/MONITOR'S REPORT NUMBER(S) 46207-EG.2		
12. DISTRIBUTION AVAILABILITY STATEMENT Approved for Public Release; Distribution Unlimited					
13. SUPPLEMENTARY NOTES The views, opinions and/or findings contained in this report are those of the author(s) and should not be construed as an official Department of the Army position, policy or decision, unless so designated by other documentation.					
14. ABSTRACT This project has designed, developed and field-tested biologically inspired strategies, algorithms and hardware for vision-based guidance of aircraft for the performance of a variety of tasks, listed below. i) Control of aircraft altitude and attitude, and terrain following are achieved by using a novel principle of 'virtual optic flow' to monitor and regulate the height and the orientation of the aircraft relative to the ground.					
15. SUBJECT TERMS Vision, aircraft, guidance, terrain following, attitude control, target detection					
16. SECURITY CLASSIFICATION OF:			17. LIMITATION OF ABSTRACT UU	15. NUMBER OF PAGES	19a. NAME OF RESPONSIBLE PERSON Michael Ibbotson
a. REPORT UU	b. ABSTRACT UU	c. THIS PAGE UU			19b. TELEPHONE NUMBER 612-612-5411

Report Title

BIOLOGICALLY INSPIRED STRATEGIES, ALGORITHMS AND HARDWARE FOR VISUAL GUIDANCE OF AUTONOMOUS HELICOPTERS

ABSTRACT

This project has designed, developed and field-tested biologically inspired strategies, algorithms and hardware for vision-based guidance of aircraft for the performance of a variety of tasks, listed below.

- i) Control of aircraft altitude and attitude, and terrain following are achieved by using a novel principle of ‘virtual optic flow’ to monitor and regulate the height and the orientation of the aircraft relative to the ground.
 - ii) Obstacle detection and avoidance are achieved by using virtual optic flow to sense and steer away from objects that are dangerously close to the flight path.
 - iii) Algorithms have been developed and tested for stabilizing and controlling aircraft attitude by monitoring the horizon profile.
 - iv) Algorithms, based on analysis of optic flow, have been developed for the detection of moving targets by a moving vision system.
-

List of papers submitted or published that acknowledge ARO support during this reporting period. List the papers, including journal references, in the following categories:

(a) Papers published in peer-reviewed journals (N/A for none)

W. Stürzl, D. Soccol, J. Zeil, N. Boeddeker, and M. V. Srinivasan (2008) Rugged, obstruction-free, mirror-lens combination for panoramic imaging. *Applied Optics* 47 (32), pp. 6070–6078. (With cover illustration).

A. Cheung, S.W. Zhang, C. Stricker, M.V. Srinivasan (2008) Animal navigation: General properties of directed walks. *Biol. Cybern.* 99, 197-217.

M.V. Srinivasan, S. Thurrowgood and D. Soccol (2009) From flying insects to autonomously navigating robots. *IEEE Robotics and Automation Magazine*, Special Issue on Cognitive Robotics. 16(3): 59-71.

P. Bhagavatula, C. Claudianos, M. Ibbotson and M. Srinivasan (2009) Edge detection in landing budgerigars (*Melopsittacus undulatus*). *PLoS ONE* 4(10): e7301.

M.V. Srinivasan (2009) Honeybees as a model for vision, perception and ‘cognition’. *Annual Review of Entomology* 55, 267–284

C. Evangelista, P. Kraft, M. Dacke, J. Reinhard and M.V. Srinivasan (2010) The moment before touchdown: Landing manoeuvres of the honeybee *Apis mellifera*. *Journal of Experimental Biology* 213, 262-270.

J. Reinhard, M. Sinclair, M. Srinivasan and C. Claudianos (2010) Honeybees learn odour mixtures via a selection of key odorants. *PLoS ONE* 5, e9110.

S. Biswas, J. Reinhard, J. Oakeshott, R. Russell, M. Srinivasan and C. Claudianos (2010) Sensory regulation of Neuroligins and Neurexin I in the honeybee brain. *PLoS ONE* 5, e9133.

D. Guez, H. Zhu, S.W. Zhang and M.V. Srinivasan (2010) Enhanced cholinergic transmission promotes recall in honeybees. *Journal of Insect Physiology* 56, 1341-1348.

C. Evangelista, P. Kraft, M. Dacke, J. Reinhard and M.V. Srinivasan (2010) The moment before touchdown: Landing manoeuvres of the honeybee *Apis mellifera*. *Journal of Experimental Biology* 213, 262-270.

M.V. Srinivasan (2010) Honeybee communication: A signal for danger. *Current Biology* 20, R366-367.

P. Kraft, C. Evangelista, M. Dacke, T. Labhart and M. V. Srinivasan (2011) Honeybee navigation: Following routes using polarized-light cues. *Phil. Trans. R. Soc. B.* 366, 703-708.

T. Luu, A. Cheung, D. Ball and M.V. Srinivasan (in press) Honeybee flight: A novel ‘streamlining’ response. *Journal of Experimental Biology*.

M.V. Srinivasan (in press) Honeybees as a model for the study of visually guided flight, navigation, and biologically inspired robotics. *Physiological Reviews*.

Book chapters

J. Reinhard and M.V. Srinivasan (2008) The role of scents in honeybee foraging and recruitment. In: *Food Exploitation by Social Insects: Ecological, Behavioral, and Theoretical Approaches*. (S. Jarau, M. Hrncir, eds.) CRC Press, Boca Raton, USA. PP. 165-182.

M.V. Srinivasan and J. Reinhard (2008) Bees: Beyond the Honey. In: *The Finlay Lloyd Book about Animals* (J. Davies, I. Hansen, eds.), Finlay Lloyd Press, Braidwood, NSW, Australia.

M.V. Srinivasan, S. Thurrowgood and D. Soccol (2009) From visual guidance in flying insects to autonomous aerial vehicles. In: *Flying Insects and Robots*, D. Floreano, J.-C. Zufferey, M.V. Srinivasan and C. Ellington (eds.), Springer- Verlag Berlin, Heidelberg, pp. 15-28.

M.V. Srinivasan, S. Thurrowgood and D. Soccol (2010) UAV guidance inspired by principles of insect vision. In: *Encyclopedia of Aerospace Engineering*, R. Blockley and W. Shyy (eds), John Wiley & Sons Ltd, Chichester, U.K. pp 4363-4374. ISBN: 9780470754405.

R.J.D. Moore, S. Thurrowgood, D. Bland, D. Soccol and M.V. Srinivasan (2011) A Bio-Inspired Stereo Vision System for Guidance of Autonomous Aircraft. In: *Advances in Theory and Applications of Stereo Vision*, Asim Bhatti (Ed.), ISBN: 978-953-307-516-7, InTech Publishers.

Number of Papers published in peer-reviewed journals: 19.00

(b) Papers published in non-peer-reviewed journals or in conference proceedings (N/A for none)

Number of Papers published in non peer-reviewed journals: 0.00

(c) Presentations

E. Middleton, M. Dacke, J. Reinhard and M. Srinivasan (2009) Flight of the Angry Bee: Target tracking and interception by aggressive honeybees. Abstract, Conference of the International Union for the Study of Social Insects (Australia), Brisbane, 3 April 2009.

E. Middleton, M. Dacke, J. Reinhard and M. Srinivasan (2009) How aggressive honeybees pursue moving targets. IBRO-ANS Advanced Neuroscience School on Neuroethology, Kioloa, 21-27 January 2009.

N. Liebsch, M.V. Srinivasan: Sticking the head into the wind: The effect of wind and the role of vision on the landing performance of honey bees. International Congress of Neuroethology, 2-7 August 2010, Salamanca, Spain, Poster abstract # 387.

T. Kornfeldt, M.V. Srinivasan, M. Dacke: Honeybee landing: is the final phase guided by stereo vision? International Congress of Neuroethology, 2-7 August 2010, Salamanca, Spain, Poster abstract # 384.

P. Bhagavatula, C. Claudianos, M. Ibbotson, M.V. Srinivasan: Head, body and wing kinematics of budgerigars (*Melopsittacus undulatus*) executing complex flight maneuvers. International Congress of Neuroethology, 2-7 August 2010, Salamanca, Spain. Poster abstract # 366.

T. Luu, A. Cheung, D. Ball, M.V. Srinivasan: Honeybee flight: A novel 'streamlining' response. International Congress of Neuroethology, 2-7 August, 2010, Salamanca, Spain, Poster abstract # 356.

M.V. Srinivasan, P. Bhagavatula, C. Claudianos, M. Ibbotson: Lateralization of obstacle avoidance in freely flying budgerigars (*Melopsittacus undulatus*). International Congress of Neuroethology, 2-7 August 2010, Salamanca, Spain. Poster abstract # 189.

M.V. Srinivasan: Visual information processing in honeybee navigation. Invited presentation, Second International Workshop on Natural Environments, Tasks and Intelligence, University of Texas, Austin, 9-11 April 2010.

M.V. Srinivasan, R. J.D. Moore, S. Thirrowgood, D. Soccol, D. Bland: Visual guidance for autonomous flight. Australian Joint Strike Fighter Advanced Technology and Innovation Conference, 3-4 May 2010.

M.V. Srinivasan: Navigating to a food source, and helping your sisters find it too. Symposium On Sensory Aspects of Pollination, The Rank Prize Funds, Grasmere, U.K., 24-27 May 2010.

M.V. Srinivasan: More than a honey machine: Vision, navigation and 'cognition' in honeybees and applications to robotics. Annual Conference of the Queensland Beekeepers' Association, Ipswich, QLD, 17-18 June 2010.

M.V. Srinivasan: Biological vision and animal navigation in the context of robotics. Annual Neuromorphic Engineering Workshop, Telluride, Colorado, 10-17 July 2010.

M.V. Srinivasan: Visual information processing in honeybee navigation and applications to robotics. Geelong Innovation Forum, Deakin University, Geelong, 1-2 November 2010.

M.V. Srinivasan: Computational principles of visual guidance in birds and bees. Fourth Australian Workshop in Computational Neuroscience, Queensland Brain Institute, University of Queensland, Brisbane, 4-5 November 2010.

Number of Presentations: 14.00

Non Peer-Reviewed Conference Proceeding publications (other than abstracts):

Peer-Reviewed Conference Proceeding publications (other than abstracts):

N. Nourani-Vatani, J. Roberts and M.V. Srinivasan (2008) IMU aided 3D visual odometry for car-like vehicles. Proceedings, Tenth Australasian Conference on Robotics and Automation, Canberra, Australia, 3-5 December 2008.

N. Nourani-Vatani, J. Roberts and M.V. Srinivasan (2009) Practical visual odometry for car-like vehicles. Proceedings, 2009 IEEE International Conference on Robotics and Automation, Kobe, Japan, May 12 - 17, 2009.

R.J.D. Moore, S. Thurrowgood, D. Bland, D. Soccol and M.V. Srinivasan (2009) A stereo vision system for UAV guidance. Proceedings, IEEE /RSJ International Conference on Intelligent Robots and Systems, 11-15 October, ST. Louis, Missouri, USA.

S. Thurrowgood, D. Soccol, R.J.D. Moore, D. Bland and M.V. Srinivasan (2009) A vision based system for attitude estimation of UAVs. Proceedings, IEEE /RSJ International Conference on Intelligent Robots and Systems, 11-15 October, ST. Louis, Missouri, USA.

R.J.D. Moore, S. Thurrowgood, D. Bland, D. Soccol and M. Srinivasan (2010) UAV altitude and attitude stabilization using a coaxial stereo vision system. In: Proceedings, IEEE International Conference on Robotics and Automation. Anchorage, Alaska, 3-8 May 2010. IEEE Press.

W. Stuerzl and M.V. Srinivasan (2010) Omnidirectional imaging system with constant elevational gain and single viewpoint. In: Proceedings, 10th Workshop on Omnidirectional Vision, Camera Networks and Sensors, Zaragoza, Spain, 27 June 2010.

S. Thurrowgood, R.J.D. Moore, D. Bland, D. Soccol and M.V. Srinivasan (2010) UAV attitude control using the visual horizon. Proceedings, Australasian Conference on Robotics and Automation (ARCA 2010), Brisbane, 1-3 December 2010. (This paper received the highest referee score).

Number of Peer-Reviewed Conference Proceeding publications (other than abstracts):

7

(d) Manuscripts

Number of Manuscripts: 0.00

Patents Submitted**Patents Awarded****Awards**

2009: Distinguished Alumni Award, Indian Institute of Science

2008: Rank Prize in Optoelectronics (U.K.)

2008: Queensland Smart State Premier's Fellowship, 2008-2012

Graduate Students

<u>NAME</u>	<u>PERCENT SUPPORTED</u>
Richard Moore	0.80
Navid Nourani	0.80
Samuel Baker	0.80
Gavin Taylor	0.70
Partha Bhagavatula	0.80
FTE Equivalent:	3.90
Total Number:	5

Names of Post Doctorates

<u>NAME</u>	<u>PERCENT SUPPORTED</u>
Dr. Peter Kraft	1.00
Dr. Nikolai Liebsch	1.00
Dr. T. Luu	0.80
FTE Equivalent:	2.80
Total Number:	3

Names of Faculty Supported

<u>NAME</u>	<u>PERCENT SUPPORTED</u>
FTE Equivalent:	
Total Number:	

Names of Under Graduate students supported

<u>NAME</u>	<u>PERCENT SUPPORTED</u>
FTE Equivalent:	
Total Number:	

Student Metrics

This section only applies to graduating undergraduates supported by this agreement in this reporting period

The number of undergraduates funded by this agreement who graduated during this period:	0.00
The number of undergraduates funded by this agreement who graduated during this period with a degree in science, mathematics, engineering, or technology fields:.....	0.00
The number of undergraduates funded by your agreement who graduated during this period and will continue to pursue a graduate or Ph.D. degree in science, mathematics, engineering, or technology fields:.....	0.00
Number of graduating undergraduates who achieved a 3.5 GPA to 4.0 (4.0 max scale):.....	0.00
Number of graduating undergraduates funded by a DoD funded Center of Excellence grant for Education, Research and Engineering:	0.00
The number of undergraduates funded by your agreement who graduated during this period and intend to work for the Department of Defense	0.00
The number of undergraduates funded by your agreement who graduated during this period and will receive scholarships or fellowships for further studies in science, mathematics, engineering or technology fields:	0.00

Names of Personnel receiving masters degrees

<u>NAME</u>
Total Number:

Names of personnel receiving PHDs

<u>NAME</u>
Total Number:

Names of other research staff

<u>NAME</u>	<u>PERCENT SUPPORTED</u>	
Dean Soccol	0.40	No
Saul Thurrowgood	0.40	No
FTE Equivalent:	0.80	
Total Number:	2	

Sub Contractors (DD882)

Inventions (DD882)

Scientific Progress

Please see attached PDF document "Final_report_DAAD19-03-1-0359_optimized.pdf"

Technology Transfer

FINAL REPORT: DAAD19-03-1-0359**VISUAL GUIDANCE OF AUTONOMOUS HELICOPTERS****INVESTIGATORS: M.V. SRINIVASAN AND M. IBBOTSON****PROJECT DURATION: 27-OCT-2008 TO 24-SEP-2009****FOREWORD**

Flying insects display remarkable agility, despite their diminutive eyes and brains. Over the past two decades there has been increasing interest in investigating how insects use their vision to stabilize flight, regulate flight speed and altitude, avoid collisions with objects, and detect and intercept other moving targets (Srinivasan, 2011) [1]. This project, funded by the US Army Research Office, is part of a larger and continuing effort in our laboratory to understand the mechanisms of visual guidance in flying insects, and to use this biological inspiration to design novel algorithms for the guidance of autonomous aerial vehicles.

TABLE OF CONTENTS

	PAGE
FOREWORD	1
TABLE OF CONTENTS	2
LIST OF ILLUSTRATIONS	3
STATEMENT OF THE PROBLEM STUDIED	5
SUMMARY OF THE MOST IMPORTANT RESULTS	6
i) Control of aircraft altitude and attitude by using ‘virtual optic flow’	6
ii) Horizon-based stabilization and control of attitude	13
iii) Detection of moving targets	16

LIST OF ILLUSTRATIONS

Figure 1 (page 7) Illustration of vision system for terrain following. (a) A video camera views the ground through a specially shaped, curved reflecting surface (b) View of system installed on the underside of a model aircraft (c) Simulation of view in the mirror as captured by the camera during horizontal flight over an infinite horizontal plane (d) Unwarped version of (c), remapped as in Fig. 3b, showing the removal of the perspective distortion along the vertical axis.

Figure 2 (page 8) Illustration of twin coaxial camera/mirror system for measuring virtual translational optic flow.

Figure 3 (page 9) (a) Test arena for calibration of the vision system (b) Virtual translational optic flow measured from the images captured by the two coaxial cameras of the vision system

Figure 4 (page 9) (a) Range as a function of (roll) view angle (blue curve and SD bars) as computed by the vision system at one cross section of the arena, compared with the true range (grey curve) (b) reconstructed terrain profile of the area, compared with the actual profile, which is represented by the boundary planes of the co-ordinate axes.

Figure 5 (page 10) Magnitude of the virtual optic flow that would be generated in the vision system by the ground during horizontal flight at zero pitch and roll.

Figure 6 (page 10) View of vision system mounted on the nose cone of a model aircraft.

Figure 7 (page 11) Comparison of pitch (upper panel) and roll (centre panel) as computed by the vision system, with the corresponding values computed from the gyroscopic signals. The bottom panel shows the altitude, as computed by the vision system.

Figure 8 (page 12) Performance of system in controlling altitude and attitude (a) Altitude (black trace) and pitch (blue trace) during periods of manual flight (white background) and automatic flight (pink background). During the *auto* mode the system is commanded to hold the aircraft at an altitude of 10 m and a pitch of 0 deg. (b) View of aircraft (left panel) and image acquired by the front camera (right panel) during an *auto* mode in which the aircraft is commanded to maintain an altitude of 15 m and a roll angle of -45 deg.

Figure 9 (page 13) Illustration of how the terrain-following vision system of Fig. 1 defines a collision-free cylinder whose radius depends upon the highest magnitude of optic flow that is measured.

Figure 10 (page 15) Insect ocellus-inspired system for measuring and stabilizing aircraft attitude by monitoring the horizon. (a) Illustration of system performance. The graphs show pitch (green trace) and roll (red trace) during the *manual* flight mode (blue trace low), and during the *auto* mode (blue trace high) when the system is commanded to hold a pitch angle of 0 deg and a roll angle of 40 deg. (b) The left-hand panel shows an image captured by the vision system when the aircraft is under automatic control and commanded to maintain the pitch and roll angles indicated above. The right-hand panel shows an animation of the orientation of the aircraft relative to the ground plane at the same instant of time.

Figure 11 (page 17) (a) Robotic gantry for testing moving object detection algorithms (b) Panoramic imaging system comprising a camera (left) and a specially profiled reflective surface (right) (c) Raw image recorded by the system (d) Unwrapped image

Figure 12 (page 17) Experimental configuration for testing the detection of a small target moving from the bottom of the image to the top (1) or from the top to the bottom (2) while the vision system itself moves continuously toward the top (i.e. in the same direction as (1))

Figure 13 (page 18) Test image sequences for detecting a small target moving from the bottom of the image to the top (upper row) and from the top to the bottom (lower row) while the vision system itself moves toward the top at a constant speed.

Figure 14 (page 18) Tests of moving target detection by a moving vision system. The graph shows the fraction of frames in which the moving target is detected for various object speeds, using (1) a DOG filter to extract optic flow contrast and (2) a DOG filter in conjunction with a model that assumes a planar background. The graph also compares the results obtained with and without the use of a scheme to predict the target location in the next frame on the basis of the measured object velocity between the previous two frames.

Figure 15 (page 19) Position errors in the detection of the location of a moving target by a moving vision system, at various object speeds. The graph shows position error (in pixels) using (1) a DOG filter to extract optic flow contrast and (2) a DOG filter in conjunction with a model that assumes a planar background.

Figure 16 (page 19) False positives in the detection of the location of a moving object by a moving vision system, at various object speeds. The graph shows position error (in pixels) using (1) a DOG filter to extract optic flow contrast and (2) a DOG filter in conjunction with a model that assumes a planar background.

Figure 17 (page 20) Input scene, with the observer moving along a linear trajectory at a constant speed. The scene contains a static object (right) and an object undergoing self-motion (left).

Figure 18 (page 20) Optic flow: the magnitudes of the computed optic flow vectors.

Figure 19 (page 21) Stereo disparity: the computed stereo disparity for the scene. Note that the objects are at about the same distance as the background plane.

Figure 20 (page 21) Moving object detection: The self-moving object is automatically detected by combining information from the measured optic flow and stereo disparity fields.

STATEMENT OF THE PROBLEM STUDIED

The aim of this project is to design, develop and field-test biologically inspired strategies, algorithms and hardware for vision-based guidance of aircraft to achieve a variety of tasks, listed below.

- i) Control of aircraft altitude and attitude, terrain following, and obstacle avoidance
- ii) Horizon-based stabilization and control of aircraft attitude
- iii) Detection of moving targets by a moving vision system, using algorithms based on analysis of optic flow.

SUMMARY OF THE MOST IMPORTANT RESULTS

i) Control of aircraft altitude and attitude by using ‘virtual optic flow’

Flying at a constant, low height above the ground is important when there is a need to perform close-up photographic exploration of terrain, or, in a military application, to evade detection by enemy radar. If the ground speed of the aircraft is known (e.g. through measurement of airspeed, or from GPS information), then, following the example of the honeybee [1, 2], the height above the ground can be computed and regulated by measuring the optic flow that is generated by the image of the ground. The optic-flow based approach is attractive because it only requires the presence of a small, inexpensive, low-resolution video camera on board. This is in contrast to traditional methods of height measurement that use heavy, bulky and power hungry instrumentation such as radar or ultrasound, radiate energy, and compromise stealth.

Optics of the vision system

During high speed flight at low altitudes, the image of the ground, as imaged by a downward-looking camera, can move at a very high velocity, complicating the measurement of optic flow. To address this problem, we have designed and developed a vision system that uses a camera and a specially shaped convex mirror profile as shown in Figs. 1a,b to achieve two objectives. They are: (i) To reduce the speed of the image of the ground to values that are low enough to permit accurate measurement; and (ii) To remove the perspective-induced distortion of different regions of the ground in front of the aircraft (see Fig. 1c). This ensures that there is no variation in image velocity along the vertical axis of the remapped image (Fig. 1d), thus promoting the accurate measurement of optic flow along this axis [3].

This way of mapping the world is similar in some respects to that achieved by the compound eyes of semi-terrestrial crabs that live on a flat substrate [4]-- although the objective in the case of the crab seems to be translate range measurements into angular measurements in the eye, rather than to measure image velocities.

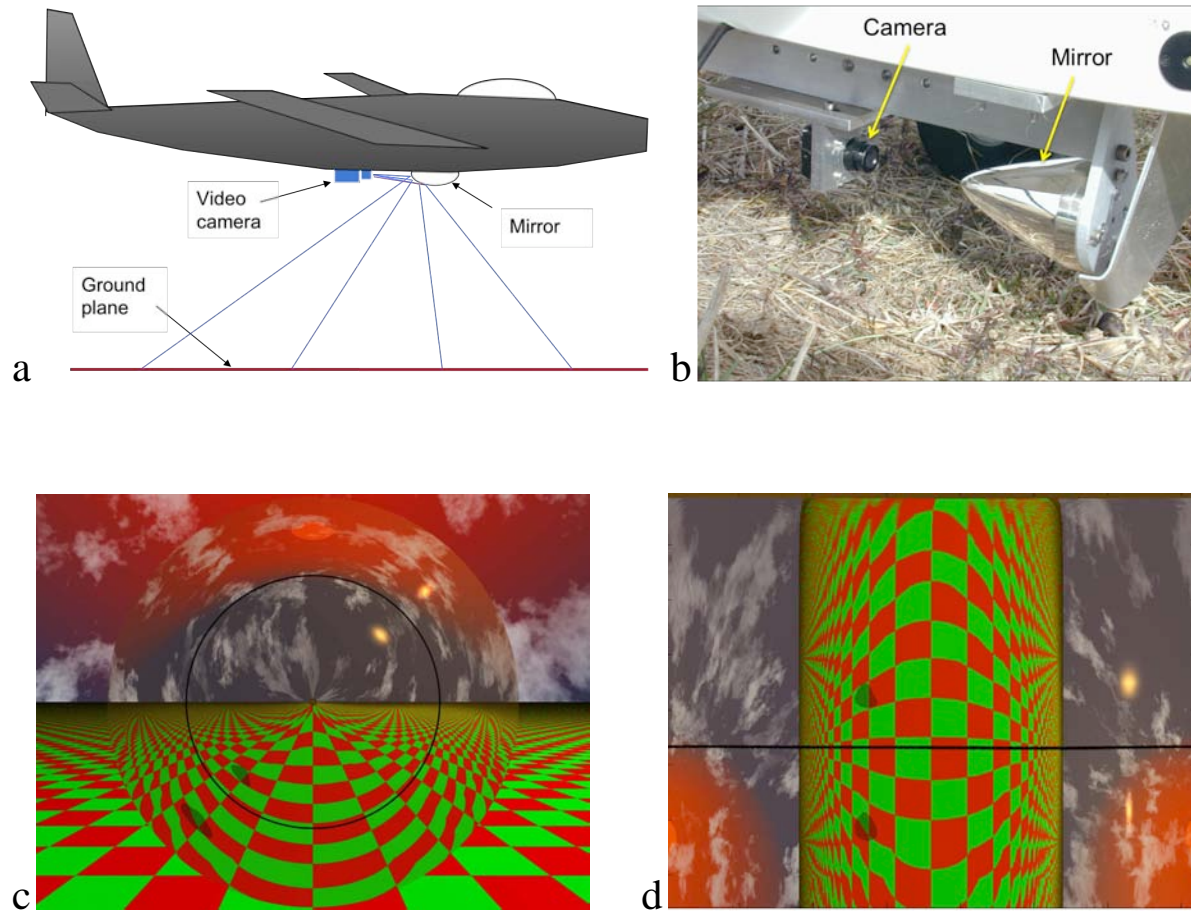


Figure 1 Illustration of vision system for terrain following. (a) A video camera views the ground through a specially shaped, curved reflecting surface (b) View of system installed on the underside of a model aircraft (c) Simulation of view in the mirror as captured by the camera during horizontal flight over an infinite horizontal plane (d) Unwarped version of (c), remapped as in Fig. 3b, showing the removal of the perspective distortion along the vertical axis.

When using optic flow to compute the range of an object, it is important to bear in mind that it is only the *translation-induced* component of optic flow that contains information on range – nearer objects induce higher magnitudes of optic flow. The flows induced by any accompanying rotations of the aircraft – for example, yaw, pitch or roll – do not carry information on range, because their magnitudes are independent of range. Consequently, we cannot work directly with the raw optic flow readings. It is necessary to (i) measure the rates of yaw, roll and pitch using gyroscopes (ii) use the gyroscopic readings in conjunction with pre-computed optic-flow templates for yaw, roll and pitch to determine the rotation-induced flow components and (iii)

calculate the translation-induced component of optic flow by subtracting, or ‘peeling off’ the flow components that are generated by the rotations. The residual pattern of optic flow, which is purely that induced by the translational component of the aircraft’s motion, can then be used compute range.

We have developed a simpler solution to the above problem. This is to artificially create the effect of a purely translatory forward motion of the aircraft by configuring *two* of the camera/mirror systems of Fig. 1, as shown in Fig. 2. The apparent optic flow that is measured by comparing the images acquired by these two systems *at the same instant of time* is then exactly equal to the flow that would have been registered by the rear mirror system if it (and the aircraft) had made a pure translation to the position of the front mirror system. The ‘virtual optic flow’ generated by this coaxially arranged, dual camera-mirror system provides an accurate and immediate reproduction of the translation-induced component of the flow, without having to move the aircraft at all. This flow can then be used for a variety of purposes, including (i) computing a range map of the environment, (ii) fitting a plane to the range data to estimate the distance and the orientation of the ground plane relative to the aircraft (iii) using this information in a feedback loop to control the aircraft’s altitude and attitude.

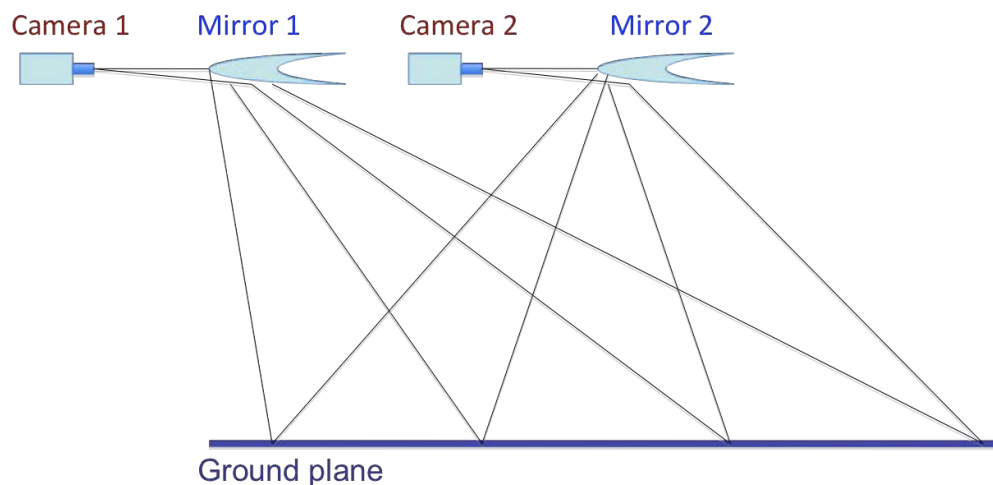


Figure 2 Illustration of twin coaxial camera/mirror system for measuring virtual translational optic flow.

Calibration of the vision system

Fig. 3a shows a view of the laboratory test arena in which the device was calibrated, and Fig. 3b shows the virtual optic flow computed between the images captured by cameras 1 and 2. Nearer points of the environment generate greater magnitudes of virtual optic flow.

Fig. 4a shows the range readings computed by the vision system for a vertical cross section of the arena, and Fig. 4b shows a reconstruction of the terrain based on the range readings. The error in the range readings is less than 5% [5] [6].

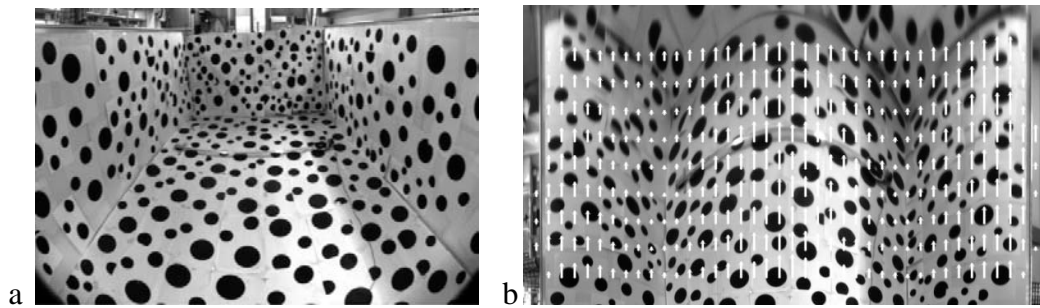


Figure 3 (a) Test arena for calibration of the vision system (b) Virtual translational optic flow measured from the images captured by the two coaxial cameras of the vision system

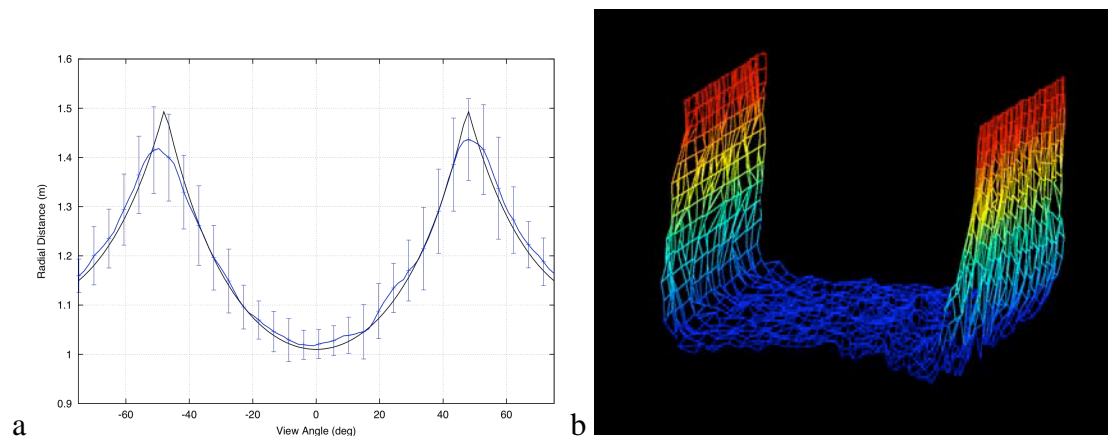


Figure 4 (a) Range as a function of (roll) view angle (blue curve and SD bars) as computed by the vision system at one cross section of the arena, compared with the true range (grey curve) (b) reconstructed terrain profile of the area, compared with the actual profile, which is represented by the boundary planes of the co-ordinate axes.

This system is used to estimate the aircraft's height above ground. If we assume the ground to be approximately planar and horizontal, we can also use the range readings to estimate the orientation of the aircraft relative to the ground, and therefore its attitude in relation to pitch and roll. Fig. 5 illustrates the magnitude profile of the virtual optic flow (or, effectively disparity) that would be generated in the vision system by the ground during horizontal flight at zero pitch and roll. The measured virtual optic flow magnitudes are fitted to a planar model of the ground to estimate the roll and pitch of the aircraft [5].

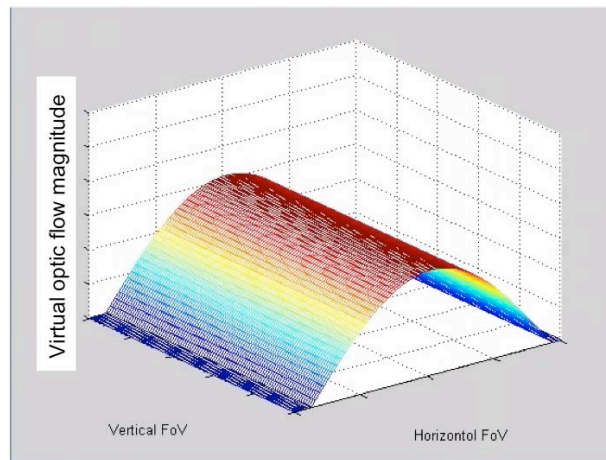


Figure 5 Magnitude of the virtual optic flow that would be generated in the vision system by the ground during horizontal flight at zero pitch and roll.

Field tests of vision system

Fig. 6 shows a view of the vision system, mounted on the nose cone of a model aircraft - a Super Frontier Senior-46 (wingspan 2040mm).

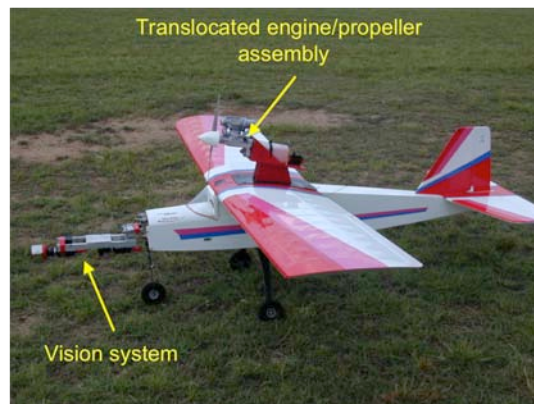


Figure 6 View of vision system mounted on the nose cone of a model aircraft

Fig. 7 shows the results of a flight test of the system. The graphs compare the roll and pitch, as computed by the vision system, with the roll and pitch as reported by the gyros. The agreement is good, allowing for the fact that gyro readings are not 100% reliable because of drift [5]. Hence, in estimating attitude the vision system that we have developed is likely to be more accurate than the gyros.

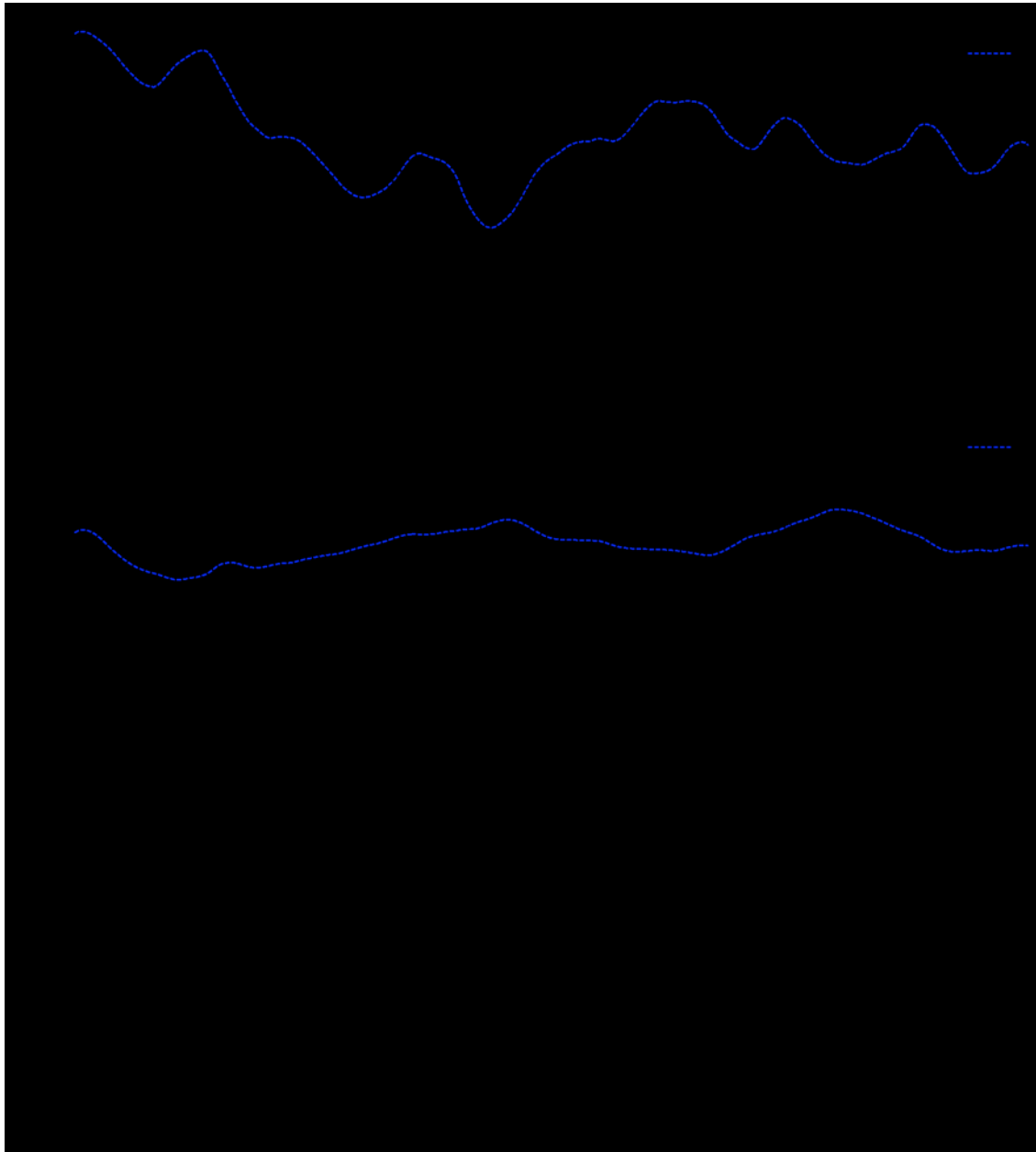


Figure 7 Comparison of pitch (upper panel) and roll (centre panel) as computed by the vision system, with the corresponding values computed from the gyroscopic signals. The bottom panel shows the altitude, as computed by the vision system.

Closed-loop control of altitude and attitude

The next step was to test the performance of the vision system in closed loop [7]. Fig. 8a shows the performance of the system in regulating altitude and attitude, where control alternates between the *manual* mode (when the aircraft is controlled by a pilot) and the *auto* mode (when the autopilot is in operation). In the *auto* mode the system is commanded to hold the altitude at 10m and the pitch at 0 deg. It is evident from Fig. 8a that the system performs these functions well. When control is passed from *manual* to *auto* at a height of 20 m and a pitch of -35 deg, the system is able to attain the target parameters within about 3 seconds. The left-hand panel of Fig. 8b is a view of the aircraft flying in a different *auto* mode where it is commanded to maintain an altitude of 15m and a roll angle of -45 deg. The right-hand panel shows an image captured by the front camera at the same instant of time.

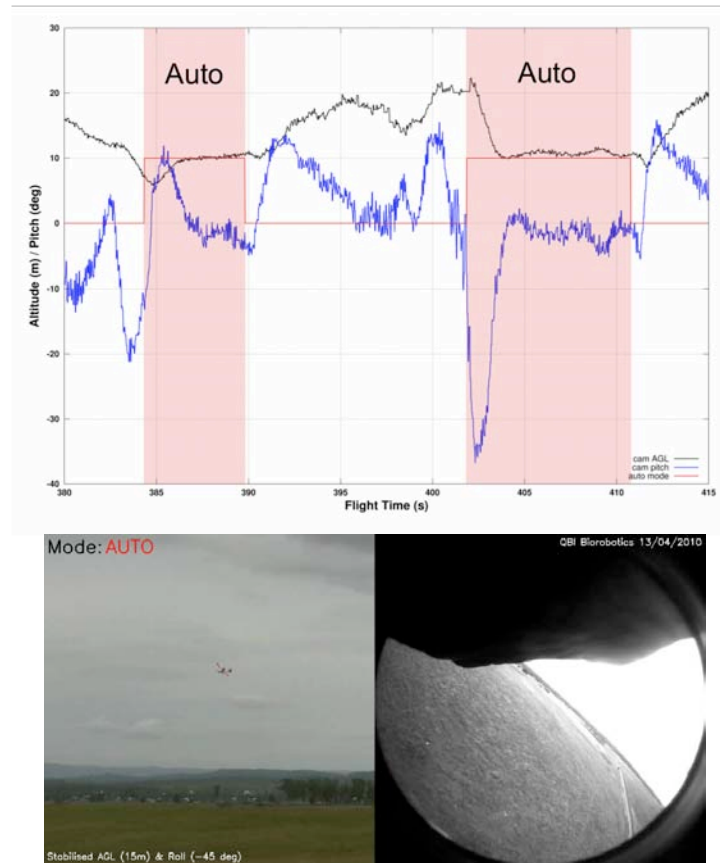


Figure 8 Performance of system in controlling altitude and attitude (a) Altitude (black trace) and pitch (blue trace) during periods of manual flight (white background) and automatic flight (pink background). During the *auto* mode the system is commanded to hold the aircraft at an altitude of 10 m and a pitch of 0 deg. (b) View of aircraft (left panel) and image acquired by the front camera (right panel) during an *auto* mode in which the aircraft is commanded to maintain an altitude of 15 m and a roll angle of -45 deg.

Obstacle detection and avoidance

The mapping performed by the mirror shown in Fig. 1 has an additional advantage: the largest magnitude of the virtual optic flow that is sensed by the system defines the radius of a ‘collision-free’ cylinder of space (a clear zone) through which the aircraft can fly safely (Fig. 9).

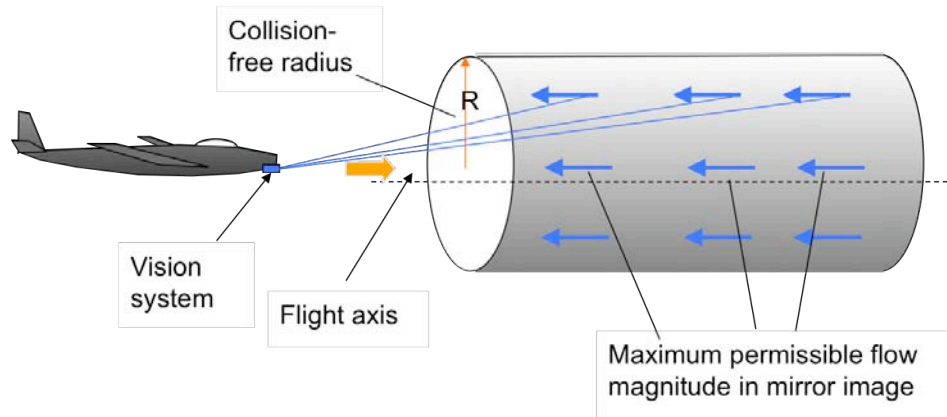


Figure 9 Illustration of how the terrain-following vision system of Fig. 1 defines a collision-free cylinder whose radius depends upon the highest magnitude of optic flow that is measured.

The smaller the flow magnitude, the larger the radius of this cylinder, and the safer the passage. Collisions with obstacles can be avoided by defining a collision-free cylinder of a prescribed radius, and computing the magnitude of optic flow corresponding to this radius. Any object that generates optic flow of a magnitude greater than this criterion value will penetrate the collision-free cylinder and be flagged as an obstacle. Control is then applied to veer away from the obstacle, thus moving it outside the cylinder [7]. An example of collision avoidance using this technique can be viewed in the movie in the accompanying Powerpoint presentation.

ii) Horizon-based stabilization and control of attitude

Conventional methods of estimating and stabilizing attitude involve the use of gyroscopes to measure the rates of roll and pitch. This approach has the disadvantage that the instantaneous attitude is determined by integrating these rates over time, which means that the error in the estimate of the attitude will increase with time, due to the presence of noise in the rate signals. The problem does not arise if the horizon is used to estimate attitude, because this visual feature

provides an absolute external reference and there is no cumulative error arising from integrating angular rates over time.

Flying insects control their attitude in roll and pitch by using three visual sensors, known as ocelli, to monitor the horizon [8] [9]. We have incorporated this principle into a vision system, as detailed below, that is capable of monitoring roll and pitch accurately and robustly, regardless of the position of the sun, clouds or other confounding factors.

We have developed an algorithm to locate the profile of the horizon in the image captured by one or more on-board cameras. The colour of each pixel in the image is analysed to determine whether it belongs to the ground or to the sky [10] [11]. This determination is carried out by generating a signal-derived variable, U , which is an optimally weighted linear combination of the R, G and B colour components of the pixel. The pixel is declared to belong to the sky or the ground according to whether U is greater or lower than a preset threshold. This procedure enhances the speed of discrimination and maximises its accuracy [11]. Horizon pixels are identified as those lying at the transition between ground and sky. The positions of these horizon pixels in the image are then back-projected into the external environment using the known geometry of the camera's optics, and a 3-D plane is fitted to these points as detailed in [11]. The orientation of this plane relative to the vision system then specifies the attitude of the aircraft relative to the horizon, thus determining its pitch and roll. This scheme is robust to the position of the sun and to changes in illumination because it locates the horizon by using information on colour, rather than intensity. A further advantage of this system is that it does not require a separate set of optoelectronic sensors for monitoring aircraft attitude – the algorithm can be incorporated into a vision system that is already place, e.g. for sensing optic flow.

The performance of this scheme is illustrated in Fig. 10a, which shows the results of a test in which the aircraft was initially flown manually, and subsequently commanded to hold a pitch angle of 0 deg and a roll angle of 40 deg during the time interval 38 – 107 sec. Manual control was resumed after 107 sec. It is evident that the aircraft maintains the prescribed attitude in a stable and accurate manner during the period of automatic control. The left-hand panel of Fig. 10b shows one frame captured by the camera during the *auto* mode, with the red line showing

the estimated horizon profile and the numbers indicating the computed values of roll and pitch. The right-hand panel of Fig. 10b shows an animated reconstruction of the instantaneous orientation of the aircraft relative to the ground plane. Recent work has demonstrated that this technique for monitoring and controlling aircraft attitude can be used to automate the execution of a variety of aerobatic manoeuvres such as loops and Immelmann turns [12].

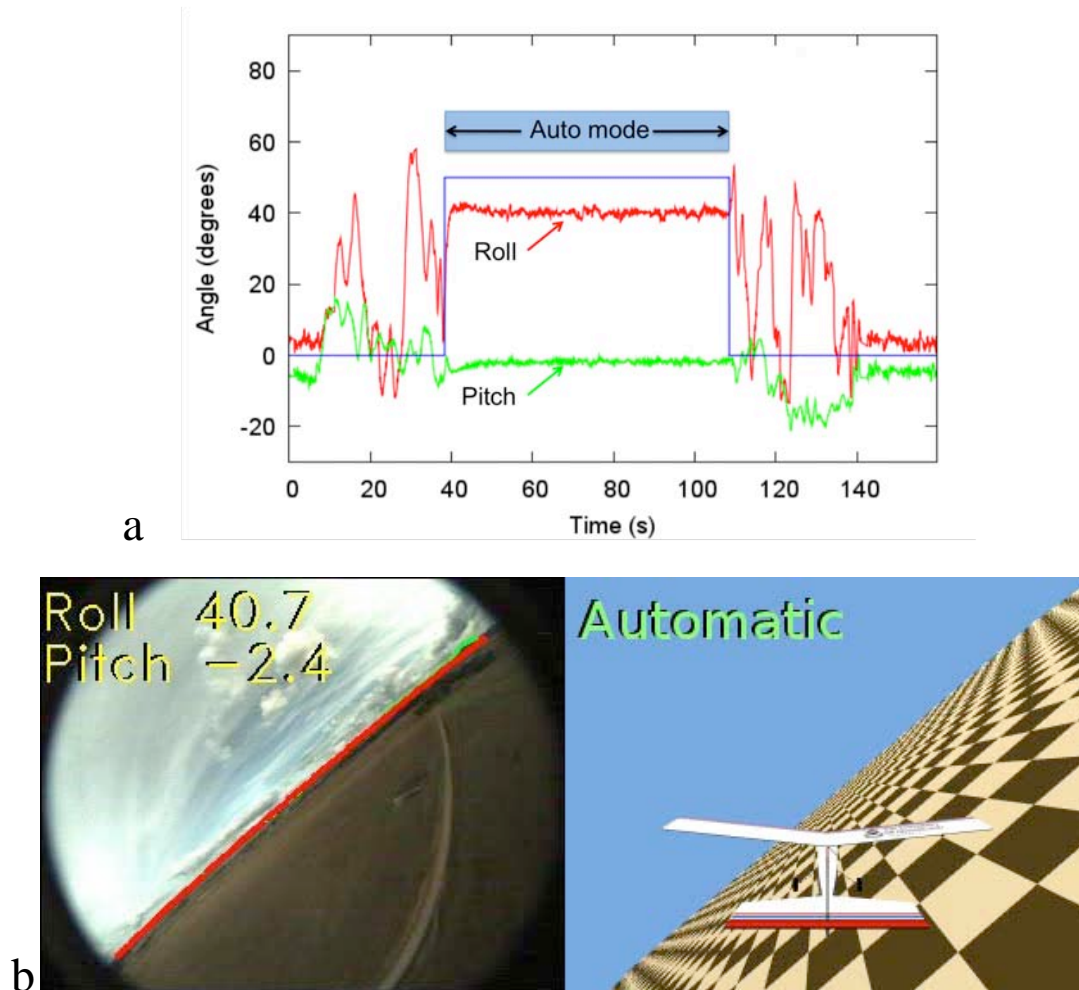


Figure 10 Insect ocellus-inspired system for measuring and stabilizing aircraft attitude by monitoring the horizon. (a) Illustration of system performance. The graphs show pitch (green trace) and roll (red trace) during the *manual* flight mode (blue trace low), and during the *auto* mode (blue trace high) when the system is commanded to hold a pitch angle of 0 deg and a roll angle of 40 deg. (b) The left-hand panel shows an image captured by the vision system when the aircraft is under automatic control and commanded to maintain the pitch and roll angles indicated above. The right-hand panel shows an animation of the orientation of the aircraft relative to the ground plane at the same instant of time.

iii) Detection of moving targets

While it is relatively straightforward to detect a moving object in a scene when the observer (or camera) is stationary – for example, through frame subtraction – this task becomes much more complex when the observer is in motion. The reason is that, when the observer moves, the images of the object as well as the background are in motion. Relative motion between the object and the background is not a reliable cue for detecting a moving object. This is because the image of a stationary object can move relative to the image of its background if the observer is undergoing translatory motion and the object is nearer to the observer than is the background.

We have developed and tested two classes of algorithms for detection of a moving target by a moving vision system.

1. One class of algorithms involves (a) measuring the optic flow field in the entire scene and (b) detecting the presence of the moving target through the motion contrast that it presents against its immediate background. This motion contrast is detected by applying a Difference-of-Gaussian (DOG) filter to the optic flow field. The technique is refined by (i) assuming a planar model for the structure of the background and (b) predicting the likely location of the target in each frame from information on its position and velocity as measured during the past two frames.

The results of this approach are shown in the next 6 figures and described in the legends.

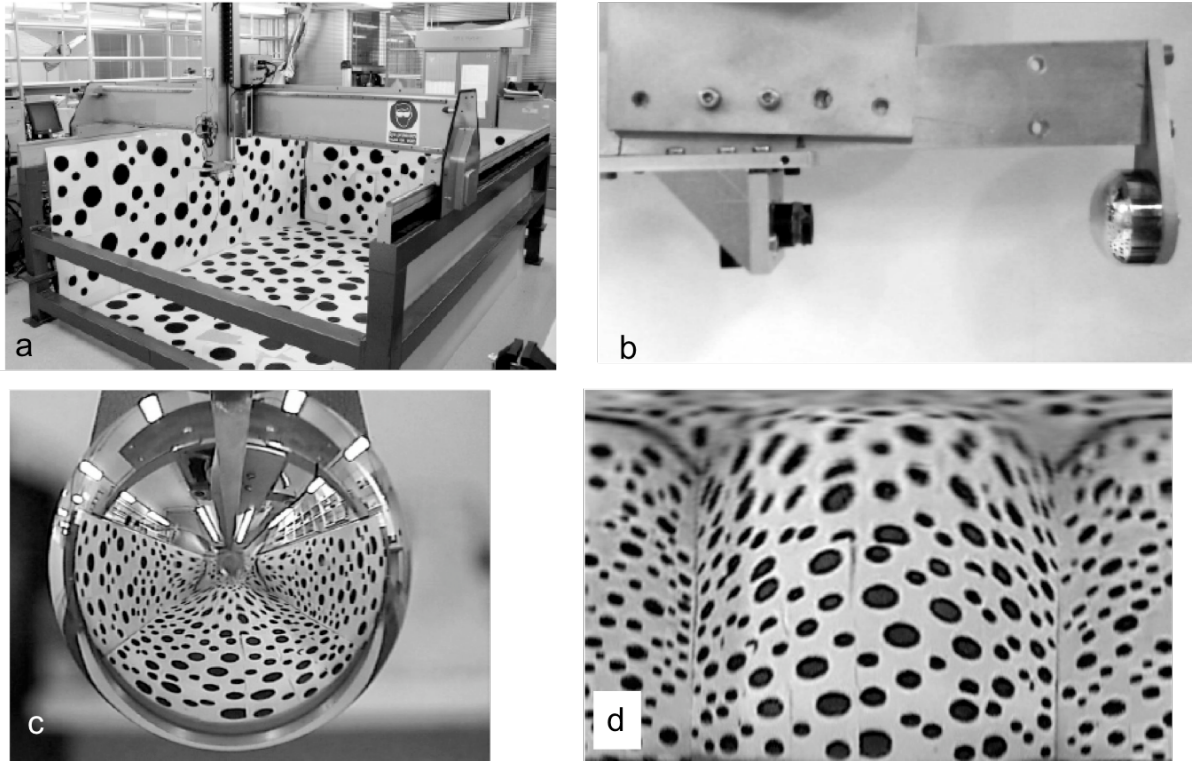


Figure 11 (a) Robotic gantry for testing moving object detection algorithms (b) Panoramic imaging system comprising a camera (left) and a specially profiled reflective surface (right) (c) Raw image recorded by the system (d) Unwrapped image

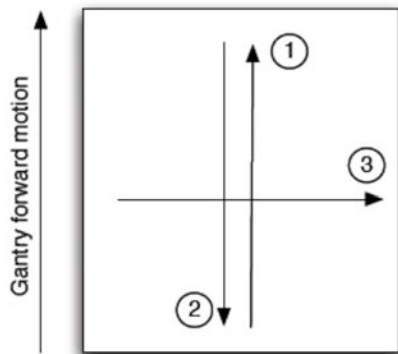


Figure 12 Experimental configuration for testing the detection of a small target moving from the bottom of the image to the top (1) or from the top to the bottom (2) while the vision system itself moves continuously toward the top (i.e. in the same direction as (1))

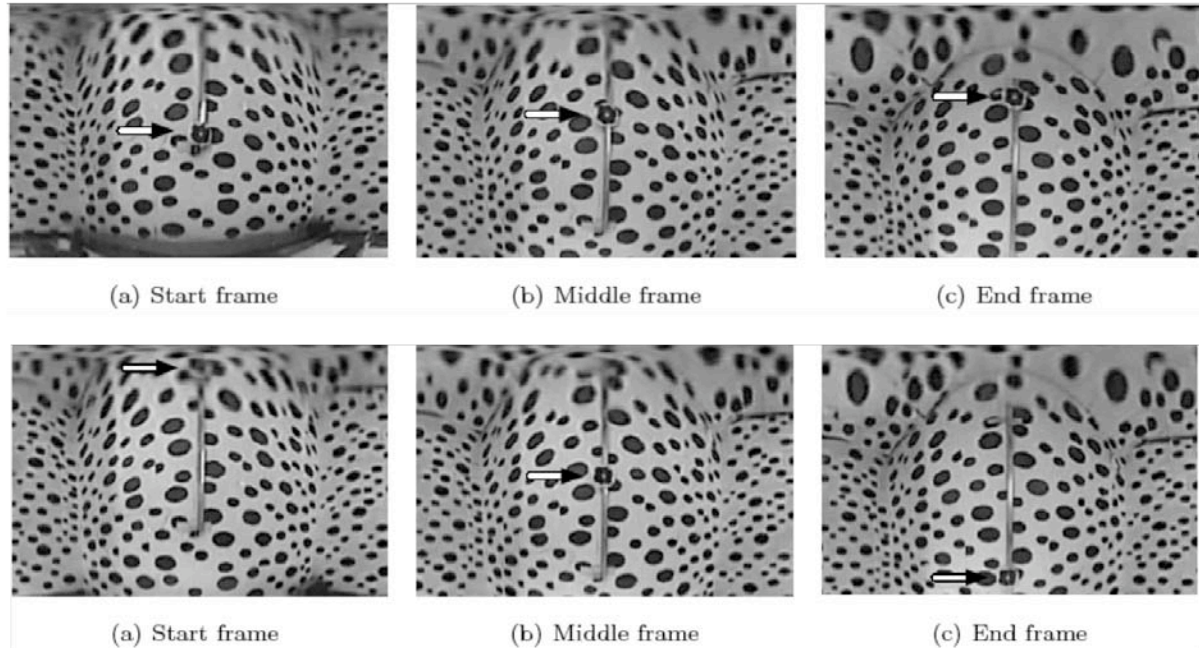


Figure 13 Test image sequences for detecting a small target moving from the bottom of the image to the top (upper row) and from the top to the bottom (lower row) while the vision system itself moves toward the top at a constant speed.

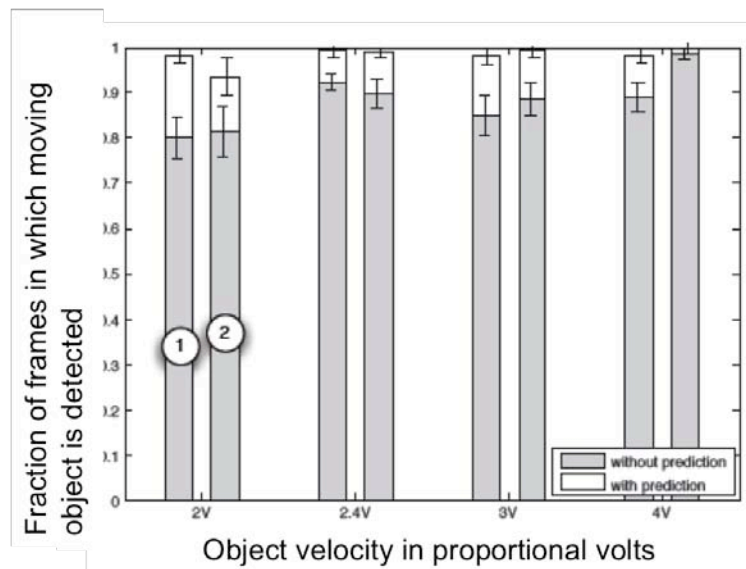


Figure 14 Tests of moving target detection by a moving vision system. The graph shows the fraction of frames in which the moving target is detected for various object speeds, using (1) a DOG filter to extract optic flow contrast and (2) a DOG filter in conjunction with a model that assumes a planar background. The graph also compares the results obtained with and without the use of a scheme to predict the target location in the next frame on the basis of the measured object velocity between the previous two frames.

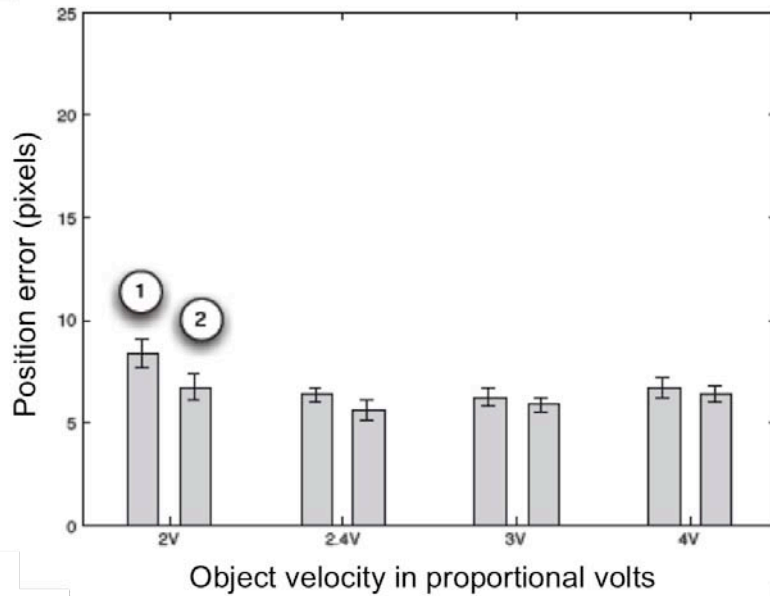


Figure 15 Position errors in the detection of the location of a moving target by a moving vision system, at various object speeds. The graph shows position error (in pixels) using (1) a DOG filter to extract optic flow contrast and (2) a DOG filter in conjunction with a model that assumes a planar background.

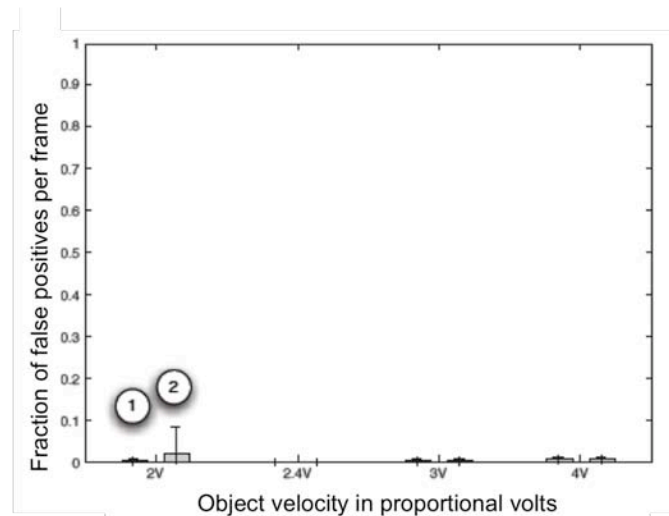


Figure 16 False positives in the detection of the location of a moving object by a moving vision system, at various object speeds. The graph shows position error (in pixels) using (1) a DOG filter to extract optic flow contrast and (2) a DOG filter in conjunction with a model that assumes a planar background.

2. A second class of algorithms that we have investigated involves (a) measuring the optic flow field that is generated in the entire scene by a pure translation of the vision system and (b) computing a range map for the entire scene using stereo vision. Moving targets are then detected as locations where the measured optic flow field vector does not match the vector that is predicted from the measured range map and the known direction of translation.

The results of this approach are shown in the next 4 figures and described in the legends.

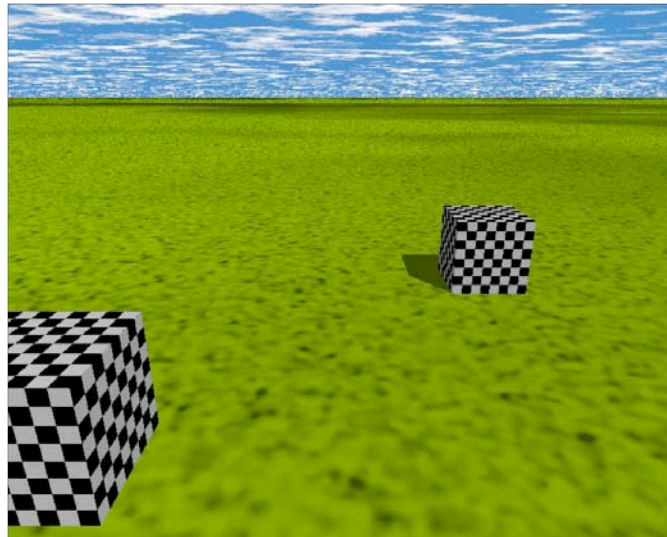


Figure 17 Input scene, with the observer moving along a linear trajectory at a constant speed. The scene contains a static object (right) and an object undergoing self-motion (left).

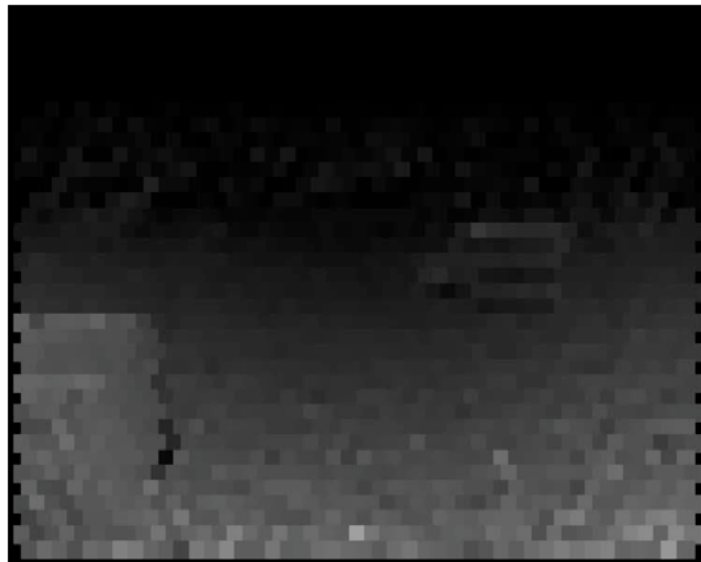


Figure 18 Optic flow: the magnitudes of the computed optic flow vectors.

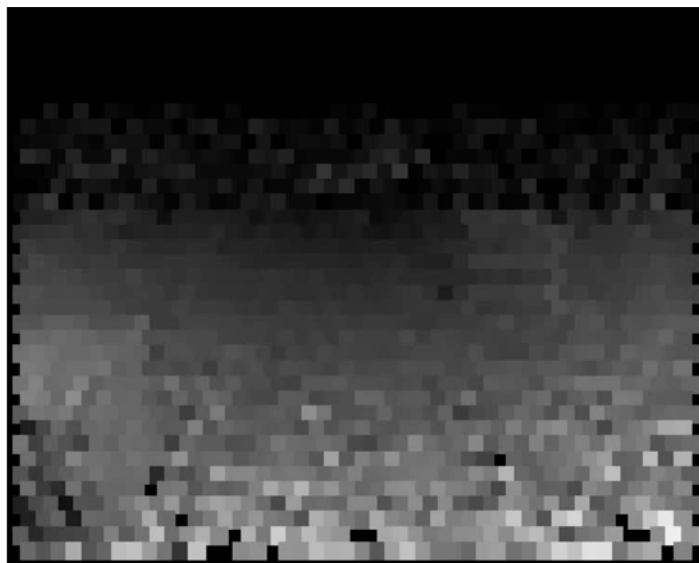


Figure 19 Stereo disparity: the computed stereo disparity for the scene. Note that the objects are at about the same distance as the background plane.

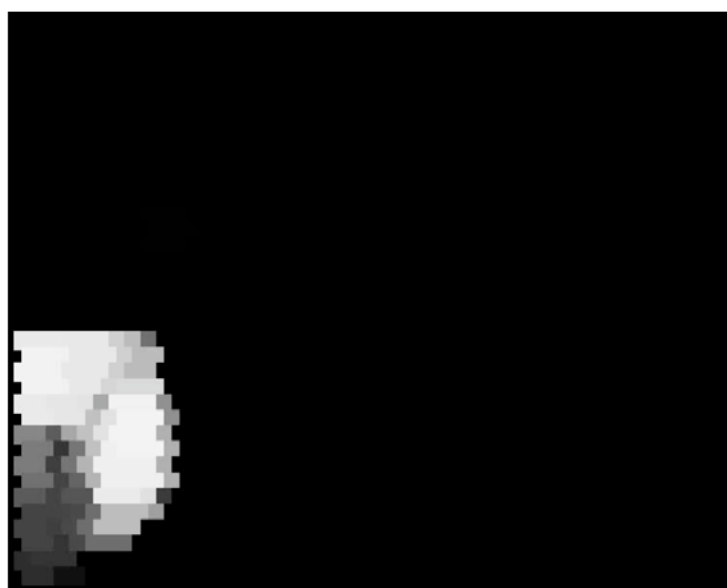


Figure 20 Moving object detection: The self-moving object is automatically detected by combining information from the measured optic flow and stereo disparity fields.

Bibliography

- [1] M. V. Srinivasan, "Honeybees as a model for the study of visually guided flight, navigation, and biologically inspired robotics", *Physiological Reviews*, vol. 91, pp. 389-411, 2011.
- [2] M. Srinivasan, S. Thurrowgood, and D. Soccol, "From flying insects to autonomously navigating robots", *IEEE Robotics and Automation Magazine*, vol. 16, pp. 59-71, 2009.
- [3] M. V. Srinivasan, S. Thurrowgood, and D. Soccol, "An optical system for guidance of terrain following in UAVs", pp. 51-56, *IEEE International Conference on Advanced Video and Signal Based Surveillance (AVSS '06)*, Sydney, 22-24 November 2006.
- [4] J. Zeil, G. Nalbach, and H.-O. Nalbach, "Eyes, eyestalks and the visual world of semi-terrestrial crabs", *J Comp Physiol A*, vol. 159, pp. 801-811, 1986.
- [5] R. J. D. Moore, S. Thurrowgood, D. Bland *et al.*, "A stereo vision system for UAV guidance", *IEEE/RSJ International Conference on Intelligent Robots and Systems*, St. Louis, Missouri, USA, 11-15 October 2009.
- [6] R. J. D. Moore, S. Thurrowgood, D. Bland *et al.*, "A bio-inspired stereo vision system for guidance of autonomous aircraft", *Advances in Theory and Applications of Stereo Vision*, A. Bhatti, ed.: InTech, 2011.
- [7] R. J. D. Moore, S. Thurrowgood, D. Bland *et al.*, "UAV altitude and attitude stabilization using a coaxial stereo vision system", *IEEE International Conference on Robotics and Automation*, Anchorage, Alaska, May 3-8, 2010.
- [8] G. Stange, "The ocellar component of flight equilibrium control in dragonflies," *Journal of Comparative Physiology*, vol. 141, pp. 335-347, 1981.
- [9] R. Berry, J. van Kleef, and G. Stange, "The mapping of visual space by dragonfly lateral ocelli," *Journal of Comparative Physiology A-Neuroethology Sensory Neural and Behavioral Physiology*, vol. 193, no. 5, pp. 495-513, May, 2007.
- [10] S. Todorovic, and M. C. Nechbya, "A vision system for intelligent mission profiles of micro air vehicles," *IEEE Transactions on Vehicular Technology*, vol. 53, no. 6, pp. 1713-1725, 2004.
- [11] S. Thurrowgood, D. Soccol, R. J. D. Moore *et al.*, "A vision based system for attitude estimation of UAVs", *IEEE /RSJ International Conference on Intelligent Robots and Systems*, ST. Louis, Missouri, USA, 11-15 October 2009.
- [12] S. Thurrowgood, R. J. D. Moore, D. Bland *et al.*, "UAV attitude control using the visual horizon", *Twelfth Australasian Conference on Robotics and Automation*, Brisbane, 1-3 December 2010.